VIBRATION ENERGY HARVESTERS OF LEAD-FREE $(K,Na)NbO_3$ PIEZOELECTRIC THIN FILMS

I. Kanno[1]*, T. Ichida[1], H. Kotera[1], K. Shibata[2], F. Horikiri[2], T. Mishima[2]
[1]Department of Micro Engineering, Kyoto University, Kyoto, Japan
[2]Hitachi Cable, Ltd., Tsuchiura, Japan
*kanno@mech.kyoto-u.ac.jp

Abstract: In this study, we fabricated piezoelectric energy harvesters composed of lead-free $(K,Na)NbO_3$ (KNN) thin films and compared the power generation performance with PZT-thin film energy harvesters. Both of the piezoelectric thin films were deposited on Pt/Ti/Si cantilevers by rf-sputtering. The KNN and PZT thin films had perovskite structure, and showed the relative dielectric constants of 744 and 872, respectively. The transverse piezoelectric properties were evaluated from the inverse piezoelectric effect and both films showed the almost the same $e_{31,f}$ of −11 C/m^2. The performance of the power generation was measured for the simple unimorph cantilevers of KNN/Si and PZT/Si. The averaged output power of KNN and PZT thin-film reached 1.1 μW and 1.0 μW, respectively. Generalized electromechanical coupling factors (GEMC) of KNN/Si and PZT/Si energy harvesters were calculated to be 1.7×10^{-3} and 0.65×10^{-3}, respectively. These results suggest that the lead-free KNN films have comparable or better performance than PZT thin films in the application of MEMS energy harvest.

Keywords: piezoelectric energy harvest, lead-free, KNN thin film, PZT thin film, MEMS

INTRODUCTION

Recently, piezoelectric vibration energy harvesting has attracted considerable attention as an autonomous energy source for microdevices, especially for wireless sensor nodes [1-4]. To integrate the energy harvest into microdevices, the energy harvesters must be highly efficient and capable of generating sufficient electric power in a limited space. Therefore, microelectromechanical systems (MEMS) energy harvesters of piezoelectric thin films have been investigated for these purposes. Because of high piezoelectric properties, $Pb(Zr,Ti)O_3$ (PZT) thin films are commonly applied not only for energy harvest, but also for a variety of piezoelectric MEMS devices.

On the other hand, PZT-based materials include toxic lead and lead-free piezoelectric devices are strongly required. Among the various lead-free piezoelectric materials, $(K,Na)NbO_3$ (KNN)-based ceramics have been intensively investigated as a promising candidate for the replacement of PZT ceramics [5]. The KNN thin films have also been investigated for the application to lead-free piezoelectric MEMS, and we have also reported that the KNN films showed large piezoelectric properties comparable to PZT thin films [6-8]. However, little have been reported on the application of KNN thin films, and furthermore, the power generation performance of the energy harvesters of lead-free KNN thin films has not been clarified yet.

In this study, we fabricated piezoelectric energy harvesters composed of KNN thin films and examined the performance of power generation. We also fabricated the PZT thin-film energy harvesters with the almost same dimension, and compared the performance between them to evaluate the possibility of the KNN films to lead-free MEMS energy harvest.

THIN FILM DEPOSITION

The KNN and PZT films were deposited on Pt/Ti/Si substrates by rf-magnetron sputtering. The substrate temperature was heated up to around 600 °C. The details of KNN and PZT deposition condition was reported in previous study [7,9]. Thickness of the KNN and PZT films was 3 μm and 2 μm, respectively. Composition of the KNN and PZT films was measured by energy dispersive x-ray analysis (EDX). The composition of K/Na and Zr/Ti in KNN and PZT thin films was 45/55 and 50/50, respectively.

The crystal structure of the KNN and PZT films were examined by x-ray diffraction (XRD) measurements, and XRD patterns of each thin film on Pt/Ti/Si substrates were shown in Fig. 1. The KNN thin films shows the preferential orientation of (100)/(001), while the PZT films shows the strong diffractions of (100)/(001) and (110). Fig. 2 shows the cross-sectional scanning electron microscope (SEM) images of KNN and PZT films. Both films had dense structure without pore or cracking.

After above measurements, we prepared unimorph cantilevers of KNN/Si and PZT/Si. Top electrodes were deposited on the surface of the KNN and PZT films, the Si substrates were cut into 3.4 mm-wide and 20 mm-long rectangular beams. The thickness of the Si substrates was 200 μm. One end of each beam was clamped by a vise, and simple unimoprh cantilevers of KNN/Si and PZT/Si were prepared. Both unimorph cantilevers had almost the same configuration, and we compared them each other.

PIEZOELECTRIC PROPERTIES

Dielectric and ferroelectric properties of KNN and PZT films were evaluated. For the measurements, circular Pt top electrodes of 3 mm in diameter were

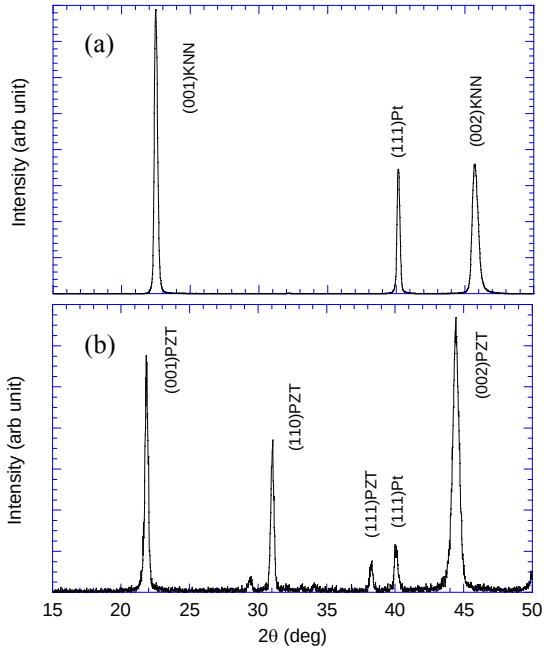

Fig. 1: XRD patterns: (a) KNN and (b) PZT thin films on Pt/Ti/Si substrates

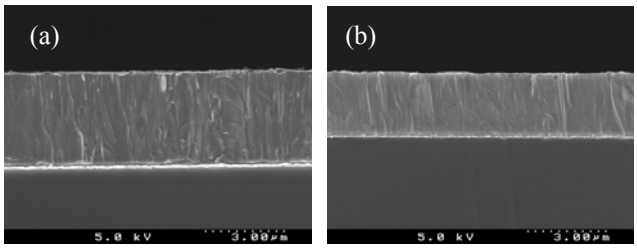

Fig. 2: Cross-sectional SEM images: (a) KNN and (b) PZT thin films

deposited on the films, and relative dielectric constant (ε_r) and dielectric loss (tanδ) were evaluated and the results are shown in Table 1. Although KNN films showed relatively large tanδ, both films had very large dielectric constant. We also evaluated the ferroelectricity by Sawer-Tower circuit, and confirmed that both films showed typical ferroelectric *P-E* hysteresis curves with remanent polarization as high as 10 μC/cm^2 and 20 μC/cm^2 for KNN and PZT thin films, respectively.

Transverse piezoelectric properties of KNN and PZT films were evaluated from the displacement of KNN/Si and PZT/Si unimorph cantilevers. The piezoelectric coefficient of $e_{31,f}$ was calculated from the following equations,

$$e_{31,f} = \frac{d_{31}}{s_{11}^{E} + s_{12}^{E}} = \frac{E_s h_s^{\,2}}{3(1-\nu_s)VL^2} \cdot \delta$$

where d_{31}, s_{11}, and s_{12} are piezoelectric coefficient and elastic compliances of the piezoelectric thin films. E_s, ν_s, h_s, are the Young's modulus, poisson's ratio and thickness of the substrate, and V, L, δ are applied voltage, length of cantilever and displacement, respectively. The focused He-Ne laser beam was shined at 13.5 mm from the fixed end of each cantilever. The displacement and $e_{31,f}$ as a function of

Table 1: Dielectric and piezoelectric properties

	KNN	PZT
ε_r	744	872
tanδ (%)	7.1	3.9
$e_{31,f}$ (C/m^2)	-8.4 ~ -11	-9.3 ~ -11.1

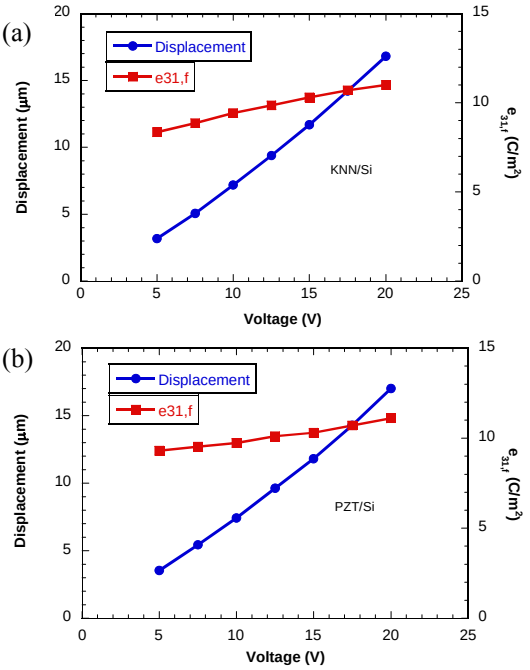

Fig. 3: Tip displacement of piezoelectric unimorph cantilevers and piezoelectric coefficient $e_{31,f}$: (a) KNN and (b) PZT thin films.

applied voltage are shown in Fig. 3. The displacement of both unimorph cantilevers proportionally increased with applied voltage. Since unimorphs of the KNN/Si and PZT/Si had almost the same configuration, the displacement represented the piezoelectric properties of the KNN and PZT films. We calculated $e_{31,f}$ from the tip displacement from 5 V to 20 V, and confirmed the large piezoelectric coefficient $e_{31,f}$ of -8.4 C/m^2 ~ -11.0 C/m^2 for KNN films, and -9.3 C/m^2 ~ -11.1 C/m^2 for PZT films, respectively. The dependence on applied voltage is attributed to the effect of domain rotation of the piezoelectric films [9]. However, the difference of $e_{31,f}$ is small so that the comparable performance of power generation is expected for KNN thin films.

POWER GENERATION

We evaluated the output power of the unimorph cantilevers of KNN/Si and PZT/Si by using the measurement setup as shown in Fig. 4. The length of the KNN/Si and PZT/Si cantilevers was 16.5 mm and 17.5 mm, respectively. The unimorph cantilever was mounted on the shaker and lead lines between top and bottom electrodes were connected to the load resistance. The voltage of the load resistance was measured as output voltage under the continuous vibration.

First, we measured frequency response of the

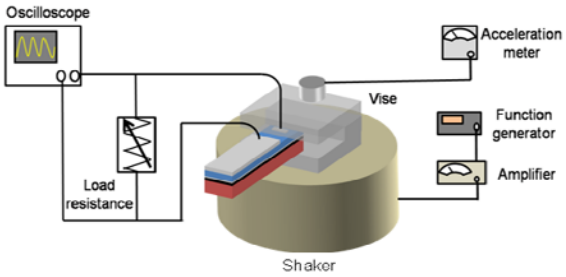

Fig. 4: Measurement setup of output power

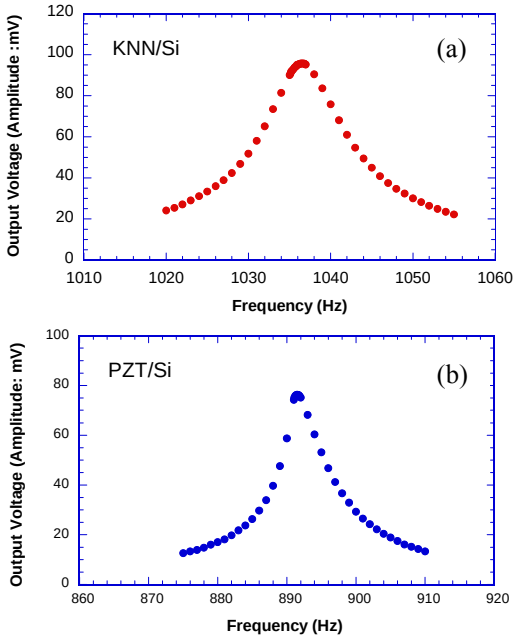

Fig. 5: Frequency response of output voltage: (a) KNN/Si and (b) PZT/Si energy harvesters

output voltage under an acceleration of 10 m/s^2 at the load resistance of 1 MΩ, and the results of both energy harvesters were shown in Fig. 6. Clear peaks of the output voltage appear at the frequency of 1036 Hz and 892 Hz for KNN/Si and PZT/Si, respectively. These frequencies are consistent with the calculated first resonance for each cantilever. The quality factor (Q) and the amplitude of maximum output voltage are listed in Table 2.

At the resonance, output voltage (v) of the simple unimorph cantilever can be calculated from the following equation [10],

$$|v| = \frac{\gamma^w d_{31} E_p h_c b Y_0}{2\varsigma C_p} \frac{d\phi_r}{dx}\bigg|_{x=L} \quad (1)$$

$$\phi_r = \sqrt{\frac{1}{mL}}\left[\cosh\frac{\lambda}{L}x - \cos\frac{\lambda}{L}x - \sigma\left(\sinh\frac{\lambda}{L}x - \sin\frac{\lambda}{L}x\right)\right] \quad (2)$$

$$\sigma = \frac{\sinh\lambda - \sin\lambda}{\cosh\lambda + \cos\lambda} \quad (3)$$

$$\gamma_w = \int_0^L \phi_r dx \quad (4)$$

where L, b, m, ς, C_p are length, width, mass of the unit length, damping ratio, and capacitance of the

Table 1: Resonant frequency and output voltage.

	KNN	PZT
Resonant frequency (Hz)	1036	892
Quality factor	120	160
Output voltage (mV)		
Experiment	96	75
Calculation	71	101

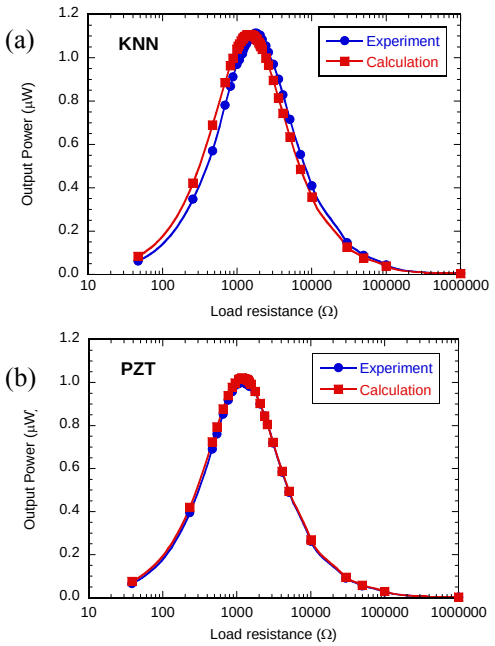

Fig. 6: Output power as a function of load resistance: (a) KNN/Si and (b) PZT/Si. Red and blue lines represent experimental and calculation, respectively

cantilever, respectively. h_c and Y_0 are distance of the neutral axis between piezoelectric film and substrate, and amplitude of external vibration. E_p and d_{31} are Young's modulus and piezoelectric coefficient of the piezoelectric thin films, respectively. At the first resonance, λ is 1.875. The Young's modulus of the KNN and PZT films was assumed to be the same as the ceramics data [11,12]. The calculated output voltage is listed in Table 2. These results indicate that although there is some deviation, output voltage of the unimorph cantilever can be predicted by the theoretical calculation on the basis of Euler-Bernoulli's assumption.

Next, we evaluated the averaged electric power output [$P = V^2/(2R)$] as a function of load resistance. The measurements were performed at the resonant frequency under the acceleration of 10 m/s^2, and the results are shown in Fig. 6. The maximum electric output power of KNN/Si and PZT/Si energy harvesters were 1.1 μW and 1.0 μW, respectively. Because both unimorph cantilevers had almost same configuration, these results imply that lead-free KNN thin films have the performance of power generation compatible with PZT films.

We consider the characteristics of the output power of KNN and PZT energy harvesters on the basis

of the electric equivalent circuit [13]. The output power at the resonance is expressed by

$$P = \frac{{\mu_1}^2 ma^2}{2\omega_0} \frac{K^2 \psi Q^2}{\psi^2 + \left(1 + K^2 \psi Q\right)^2} \quad (5)$$

where m, a, ω, and Q are the cantilever's effective mass, acceleration, fundamental mechanical angular frequency, and mechanical quality factor. K represents the generalized electromechanical coupling factor (GEMC), and ψ is the normalized mechanical resonant frequency expressed by

$$\Psi = \omega_0 RC \quad (6)$$

where C is the capacitance of the energy harvester. In this study, since we did not attach a seismic mass on the cantilever, the correction factor μ_1(=1.566) is applied to Eq. (5) [10]. By Eq. (5), we calculated GEMC by fitting the experimental results. Blue lines in Fig. 6 represent the calculated output power when K2 of KNN/Si and PZT/Si energy harvesters are 1.7×10^{-3} and 0.65×10^{-3}, respectively. GEMC is important parameter to determine output power of piezoelectric energy harvesters and maximum output power of KNN/Si was higher than that of PZT/Si. On the other hand, it is reported that $e_{31,f}$ of the PZT films reaches -17 C/m^2 [14], it is expected that the output power of PZT/Si might be enhanced by improving piezoelectric properties of PZT films. Taking these results into consideration, the KNN thin-film energy harvesters have comparable or higher performance than those of PZT thin films.

In this study, we used simple unimorph structure to evaluate the fundamental characteristics of lead-free KNN films. Therefore, resulting output power and GEMC were relatively smaller than those of the other piezoelectric MEMS energy harvesters ever reported. However, we can easily expect that the output power of KNN thin-film (and PZT thin-film) energy harvesters can be enhanced by attaching seismic mass at the tip of the cantilevers, and further optimization of the design and structure of them.

CONCLUSIONS

We fabricated piezoelectric energy harvesters composed of lead-free KNN thin films and compared the performance of power generation with PZT thin-film energy harvesters. The KNN and PZT films were deposited on Pt/Ti/Si substrates by rf-sputtering. The KNN and PZT films have excellent piezoelectric coefficient $e_{31,f}$ of −8.4 ~ −11.0 C/m^2 and −9.3 ~ −11.0 C/m^2, respectively. The energy harvesters of KNN thin films showed the maximum output power of 1.1 μW, while that of PZT thin films showed 1.0 μW. Taking the variation of piezoelectric properties and dielectric properties of KNN and PZT films, lead-free KNN energy harvesters have the comparable performance to conventional PZT MEMS energy harvesters.

REFERENCES

[1] K. A. Cook-Chennault, N. Thambi, A. M. Sastry, 2008 Powering MEMS portable devices—a review of non-regenerative and regenerative power supply systems with special emphasis on piezoelectric energy harvesting systems, *Smart Mater. Struct.* **17** 043001

[2] S. P. Beeby, M. J. Tudor, N. M. White, 2006 Energy harvesting vibration sources for microsystems applications, *Meas. Sci. Technol*. **17** R175-R195

[3] H.-U. Kim, W.-H. Lee, H. V. Rasika Dias, S. Priya, 2009 Piezoelectric Microgenerators--Current Status and Challenges, *IEEE Trans. Utrason. Ferroelectr. Freq. Control* **56** 1555-1568

[4] S. Roundy, P. K. Wright, 2004 A piezoelectric vibration based generator for wireless electronics, *Smart Mater. Struct*. **13** 1131

[5] Y. Saito, H. Takao, T.Tani, T. Nonoyama, K. Takatori, H. Homma, T. Nagaya, M. Nakamura, 2004 Lead-free piezoelectric ceramics, Nature **432** 84-87

[6] I. Kanno, T. Mino, S. Kuwajima, T. Suzuki, H. Kotera, K. Wasa, 2007 Piezoelectric Properties of (K,Na)NbO_3 Thin Films Deposited on (001)$SrRuO_3$/Pt/MgO Substrates, *IEEE Trans. Ultrason., Ferroelectr., Freq. Control.*, 54, 2562-2566

[7] K. Shibata, F. Oka, A. Ohishi, T. Mishima, I. Kanno, 2008 Piezoelectric properties of (K,Na)NbO_3 films deposited by RF magnetron sputtering, *Appl. Phys. Express*, **1** 011501

[8] K. Shibata, K. Suenaga, K. Watanabe, F. Horikiri, A. Nomoto, T. Mishima, 2011 Improvement of piezoelectric properties of (K,Na)NbO_3films deposited by sputtering, Jpn. J. Appl. Phys. **50** 041503

[9] I. Kanno, H. Kotera, K. Wasa, 2003 Measurement of transverse piezoelectric properties of PZT thin films, *Sens. Actuators A*, **107**, 68-74

[10] A. Erturk, D. J. Inman, 2008 On mechanical modeling of cantilevered piezoelectric vibration energy harvesters, *J. Intell. Mater. Syst. Struct.* **19** 1311-1325

[11] L. Egerton, D.M. Dillon, 1959 Piezoelectric and dielectric properties of ceramics in the system potassium-sodium niobate, *J. Am. Ceram. Soc*. **42** 438-442

[12] D.A. Berlincourt, C.Cmolic, H. Jaffe, 1960 Piezoelectric properties of polycrystalline lead titanate zirconate compositions, *Proc. IRE*, 220-2209

[13] M. Renaud, K. Karakaya, T. Sterken, P. Fiorini, C. Van Hoof, R. Puers, 2008 Fabrication, modelling and characterization of MEMS piezoelectric vibration harvesters, *Sens.Actuators A* **145-146** 380-386

[14] P. Muralt, 2008 Recent progress in materials issues for piezoelectric MEMS, *J. Am. Ceram. Soc*. 91 1385-1396